



Deposited via The University of York.

White Rose Research Online URL for this paper:

<https://eprints.whiterose.ac.uk/id/eprint/532/>

Article:

Ritchie, A.V., Fouquet, C., Alvarez-Curto, E. et al. (2005) Evolutionary origin of cAMP-based chemoattraction in the social amoebae. *Proceedings of the National Academy of Sciences of the United States of America*. pp. 6385-6390. ISSN: 1091-6490

<https://doi.org/10.1073/pnas.0502238102>

Reuse

Items deposited in White Rose Research Online are protected by copyright, with all rights reserved unless indicated otherwise. They may be downloaded and/or printed for private study, or other acts as permitted by national copyright laws. The publisher or other rights holders may allow further reproduction and re-use of the full text version. This is indicated by the licence information on the White Rose Research Online record for the item.

Takedown

If you consider content in White Rose Research Online to be in breach of UK law, please notify us by emailing eprints@whiterose.ac.uk including the URL of the record and the reason for the withdrawal request.

Evolutionary origin of cAMP-based chemoattraction in the social amoebae

Elisa Alvarez-Curto*, Daniel E. Rozen*[†], Allyson V. Ritchie*, Celine Fouquet*, Sandra L. Baldauf[‡], and Pauline Schaap*[§]

*School of Life Sciences, University of Dundee, Dundee DD1 5EH, United Kingdom; and [‡]Department of Biology, University of York, P.O. Box 373, York YO10 5YW, United Kingdom

Communicated by J. T. Bonner, Princeton University, Princeton, NJ, March 22, 2005 (received for review January 18, 2005)

Phenotypic novelties can arise if integrated developmental pathways are expressed at new developmental stages and then recruited to serve new functions. We analyze the origin of a novel developmental trait of Dictyostelid amoebae: the evolution of cAMP as a developmental chemoattractant. We show that cAMP's role of attracting starving amoebae arose through recruitment of a pathway that originally evolved to coordinate fruiting body morphogenesis. Orthologues of the high-affinity cAMP receptor (cAR), cAR1, were identified in a selection of species that span the Dictyostelid phylogeny. The cAR1 orthologue from the basal species *Dictyostelium minutum* restored aggregation and development when expressed in an aggregation-defective mutant of the derived species *Dictyostelium discoideum* that lacks high-affinity cARs, thus demonstrating that the *D. minutum* cAR is a fully functional cAR. cAR1 orthologues from basal species are expressed during fruiting body formation, and only this process, and not aggregation, was disrupted by abrogation of cAR1 function. This is in contrast to derived species, where cAR1 is also expressed during aggregation and critically regulates this process. Our data show that coordination of fruiting body formation is the ancestral function of extracellular cAMP signaling, whereas its derived role in aggregation evolved by recruitment of a preexisting pathway to an earlier stage of development. This most likely occurred by addition of distal cis-regulatory regions to existing cAMP signaling genes.

cAMP signaling | *Dictyostelium* | gene recruitment

The origin of species diversity is the story of the origin of novel features. These can arise through the development of entirely new genes (1) or when pathways underlying existing functions are coopted to perform new ones through altered regulation of the component genes. Novel features of development, which can cause dramatic shifts in species form, are particularly thought to arise in this manner (2–4). However, few data exist to support this common view and even fewer to document the steps involved at high phylogenetic and molecular genetic resolution. Here we report on the analysis of the derived origin of a novel, even group-defining, feature of Dictyostelid social amoebae: the origin of cAMP-based chemoattraction.

The Dictyostelid amoebae are a diverse group of organisms that display conditional multicellularity with a range of phenotypes (5). In the model system *Dictyostelium discoideum*, extracellular cAMP pulses coordinate the aggregation of starving amoebas (6) and are also implicated in the subsequent formation of migrating slugs and culminating fruiting structures (7). cAMP is produced by an adenyl cyclase A (8), and degraded by an extracellular phosphodiesterase, PdsA (9). Together with cAR1 or cAR3, two of the four *D. discoideum* cARs, these enzymes are essential for oscillatory cAMP signaling (10).

A molecular phylogeny of the Dictyostelids based on small subunit RNA and α -tubulin sequences shows subdivision of all known species into four major groups. *D. discoideum* lies within the most-derived Group 4, which is nested within a series of three progressively deeper lineages, the most basal of which is Group 1, the taxon closest to the outgroup of solitary amoebae (P.S. and

S.L.B., unpublished work). We selected four species, *Dictyostelium fasciculatum*, *Polysphondylium pallidum*, *Dictyostelium minutum*, and *Dictyostelium rosarium*, for study as representatives of Groups 1–4, respectively. Similar to *D. discoideum* and other investigated group four species, *D. rosarium* uses cAMP as attractant. However, none of the other species do: *D. minutum* uses folate (11); *P. pallidum*, glonin (12); and *D. fasciculatum*, an unknown compound to aggregate (5).

To unravel the evolutionary history of extracellular cAMP signaling, we searched for cAR genes in the four representative species and investigated their role in aggregation and multicellular development of these species. We also studied whether they encode fully functional cARs by heterologous expression in a *D. discoideum car1car3* double null mutant. Our studies indicate a conserved ancestral role for extracellular cAMP signaling in fruiting body morphogenesis and a derived role in aggregation.

Methods

Cell Lines and Culture. *D. minutum* 71-2, *D. fasciculatum* SH3, *P. pallidum* TNS-C-98, and *D. rosarium* M45 cells were grown in association with *Klebsiella aerogenes* on 0.1% lactose-peptone agar (5). *D. discoideum* cells were grown in HL5 medium (13). For developmental time courses, cells were harvested while in exponential phase and incubated at 22°C and 8×10^5 cells per cm² on nonnutrient agar (1.5% agar in 10 mM phosphate buffer, pH 6.5). Approximately 20 activated charcoal pellets were placed in the lids of the agar plates to promote synchronous development.

Gene Identification. The degenerate oligonucleotides, 5'-GGTAGTTTCGCATGYTGGYTNTGGAC-3' and 5'-TCACCGAAGTATCGCCACATNTRNGGRTT-3', designed to match amino acid sequences GSFACWLWT and NPLM-WRYFG that are conserved between cARs 1–4 of *D. discoideum*, were used to amplify putative cAR genes by touchdown PCR (14) from genomic DNAs of the four test species. The touchdown protocol started with four cycles with annealing at 60°C for 30 s, 10 cycles with an annealing temperature decrement of 1°C, and 20 cycles with annealing at 50°C. The PCR products were subcloned in the pGEM-T Easy vector (Promega), and their sequence was determined from at least three independent clones. The DmcAR PCR product was used to screen an λ ZapII library of sheared *D. minutum* gDNA, which was custom-made by Stratagene from *D. minutum* 71-2 genomic DNA provided by us. Three positive plaques, C2, C6, and C10, were identified, and their pBluescript phagemids were isolated by *in vitro* excision according to the manufacturer's instructions. The respective

Abbreviations: cAR, cAMP receptor; mlBP, maximum likelihood bootstrap percentage.

Data deposition: The sequences reported in this paper have been deposited in the GenBank database [accession nos. AY839643 (DrcARI), AY839644 (DrcARII), AY518271 (DmcAR), and AY518272 (DfcAR)].

[†]Present address: Department of Biology, Emory University, 1510 Clifton Road, Atlanta, GA 30322.

[§]To whom correspondence should be addressed. E-mail: p.schaap@dundee.ac.uk.

© 2005 by The National Academy of Sciences of the USA

3.5-, 4.7-, and 1.25-kb inserts were sequenced to 4-fold coverage by primer walking. The sequences could be assembled into a 4,873-bp contig, which apart from the DmcAR, contained two other ORFs. BLAST searches of the entire GenBank database showed that one partial ORF was most similar to *D. discoideum* SpkA (15) and the other complete ORF to the putative *D. discoideum* protein DDB0217155 (<http://dictybase.org>). The *D. minutum* protein was called DtmA for its only structural feature of dual transmembrane helices.

RNA Isolation and Analysis. Total RNA was isolated from 2×10^7 cells, size-fractionated on 1.5% agarose gels containing 2.2 M formaldehyde (16), and transferred to nylon membranes. Cells in the culmination stages were vortexed for 5 min with glass beads during RNA extraction to break stalk cells and spores. Membranes were hybridized at 65°C to [³²P]dATP-labeled DNA probes and washed at high stringency according to standard procedures (17). Three microliters of 0.28- to 6.6-kb RNA markers (Promega) were run on the same gel and stained with ethidium bromide to estimate the size of the cAR mRNAs.

Heterologous Expression of DmcAR. A 1,525-bp fragment was amplified from λZAPII clone C6 by using oligonucleotides 5'-CCAGATCTAAAATGGAACAATCACCCGATG-3' and 5'-CCAGATCTCAACCCCAAACCAACAAC-3' that will generate BglII restriction sites. This fragment includes the complete 1,161-bp coding region of DmcAR with 3 bp of the 5' untranslated region (UTR) and 364 bp of the 3' UTR. The BglII digested product was subcloned into the BglII site of vector PJK1 (8), which placed DmcAR downstream of the *D. discoideum* actin15 promoter and yielded vector A15:DmcAR. The integrity of the A15:DmcAR fusion was verified by DNA sequencing. The *D. discoideum car1car3* mutant (18) was transformed with either A15:DmcAR or A15:DdcAR1 in PJK1 (19) and selected for growth at 20 μg/ml G418.

cAMP-Binding Assay. To measure cell surface cAMP-binding activity, 1.6×10^7 cells were incubated for 1 min at 0°C with 1 or 10 nM [³H]cAMP (Amersham Pharmacia)/5 mM DTT/variable concentrations of cAMP in a total volume of 100 μl. Cells were separated from unbound [³H]cAMP by centrifugation for 10 s at 16,000 × *g* through a 4:11 mix of AR200:AR20 silicon oil (Wacker-Chemie, Burghausen, Germany). The [³H]cAMP associated with the cell pellet was measured by liquid scintillation counting.

Phylogenetic Analysis. For the cAR protein tree, sequences were aligned with CLUSTALX (20) by using default parameters. Only ungapped regions (or those with small gaps in single sequences) flanked by 70% consensus sites were used. The tree shown was derived by maximum likelihood and Bayesian inference analyses on 291 unambiguously aligned amino acid positions. The Bayesian inference utilized MRBAYES, Ver. 3.0 (21), with posterior probabilities values estimated from 10^7 chains and discarding a burnin of 1,000. Maximum likelihood bootstrap percentage (mlBP) values were determined from 500 replicates by using the PROML program from the PHYLIP package (22). Both analyses used the JTT model (23) for weighting amino acid substitutions and a γ correction for rate variation among sites. An α value of 1.39 was used for the γ distribution in the mlBP analyses, as determined by the program TREE-PUZZLE (24). Support values for the cAR + TasA subtree were determined from a dataset consisting of only these nine sequences to avoid loss of resolution due to long-branch attraction to the distantly related outgroup sequences. The full dataset of 13 sequences was then used to test the deeper nodes. Four G protein-coupled receptor sequences were used to root the tree, because these were shown to be the

most conservative (relative to the cAR sequences) based on phylogenetic analyses using a range of cAR-related sequences.

For the small subunit rRNA tree, complementary DNA sequences were aligned by eye, and only unambiguously aligned ungapped regions were used to construct the tree. Both Bayesian inference and maximum likelihood analyses utilized the general-time-reversible model with a γ correction for rate variation among sites and a designated proportion of invariant sites (GTR + I + G). The Bayesian inference with posterior probabilities values were estimated from 10^7 chains with a burnin of 10,000 and mlBP values from 100 replicates. All parameters were estimated from the data by the respective phylogenetic programs.

Results

Identification of cAR-Like Sequences in Four Dictyostelid Species.

Degenerate oligonucleotide primers were designed to match amino acid sequences that are conserved between the four homologous *D. discoideum* (*Dd*) cARs 1–4. These primers were used to amplify cAR-like sequences by touch-down PCR from genomic DNAs of the four test species, *D. fasciculatum*, *P. pallidum*, *D. minutum*, and *D. rosarium*. Single cAR-like sequences were obtained from *D. fasciculatum* (*DfcAR*), *P. pallidum* (*PpcAR*), and *D. minutum* (*DmcAR*) and dual sequences from *D. rosarium* (*DrcARI* and *DrcARII*). The sequences varied in size due to a variable-length intron, present in all sequences except *DmcAR*. These introns were located at the same conserved position as the single intron in *D. discoideum* cAR1–4. The derived amino acid sequences of the cAR genes showed 71–87% identity with DdcAR1 (Fig. 1*A*). *PpcAR* was identical to TasA, a putative receptor from *P. pallidum* (25). Phylogenetic analysis showed that *DfcAR*, *DmcAR*, *PpcAR*, *DrcARI*, and *DdcAR1* represent the ancestral cAR receptor lineage from which cAR2–4 were derived, including *DrcARII*, which is specifically related to DdcAR2 (Fig. 1*B*). The cAR phylogeny closely mirrors the small subunit RNA phylogeny of the five species (Fig. 1*C*), albeit that in both trees, the nodes that define the relative positions of *P. pallidum* and *D. fasciculatum* are less well resolved than the other nodes.

Developmental Regulation of cAR Expression. To assess the developmental role of the putative cARs, we hybridized [³²P]dATP-labeled DNA probes for each cAR to Northern blots of total RNA isolated during the life cycles of the four species. A *D. discoideum* developmental time course was included for comparison. Fig. 2 shows that in the most basal species *D. fasciculatum* and *P. pallidum*, a single cAR mRNA appears after aggregation is completed. This mRNA remains present until fruiting bodies have formed. *D. minutum* expresses two cAR transcripts, a smaller mRNA that occurs during growth and then decreases and a larger mRNA that appears after aggregation and persists up to fruiting body formation. *DrcARI* also yields two different size transcripts, but here, as for its close relative *DdcAR1* (26, 27), the smaller mRNA species appears just before aggregation, whereas the larger species appears after aggregation is completed. As is the case for the more basal Dictyostelids, the postaggregative mRNA remains present until fruiting bodies have formed. In case of *DrcARI*, the smaller mRNA species also persists. Because both hybridization and washing of the Northern blots were performed at high stringency, the additional bands are unlikely to result from nonspecific hybridization to other cAR genes. Expression of two mRNA species from a single gene was previously demonstrated for DdcAR1 (26). The cAR mRNAs varied between 1.4 and 2.1 kb in size; however, even the smallest 1.4-kb mRNA of *D. minutum* is large enough to accommodate the complete 1.16-kb *DmcAR* coding region (see next paragraph). We could not detect any mRNA hybridizing to the

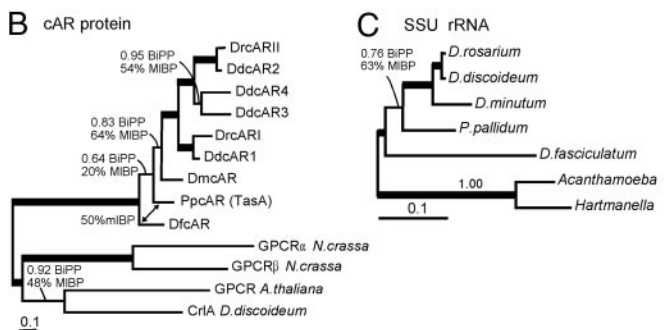


Fig. 1. Identification of cAR-like sequences in four Dictyostelid species. (A) Alignment of cAR-like sequences from four test species with the *D. discoideum* cARs. DNA fragments of 543–627 bp were amplified from *D. fasciculatum*, *D. minutum*, *P. pallidum*, and *D. rosarium* genomic DNA by using degenerate oligonucleotides that match conserved sequences in the four *D. discoideum* cARs. After excision of a variable length intron at a conserved position (arrow), the derived amino acid sequences were determined and aligned by using CLUSTAL-x. Amino acid residues that are identical in the majority or at least four of the nine sequences are shaded gray. The conserved regions used for oligonucleotide design are shown for DdcAR1–4, for PpcAR, which is identical to TasA (24), and for DmcAR. The positions of the putative transmembrane (TM) domains 3–7 of DdcAR1 (35) are indicated. GenBank accession nos: A41238 (DdcAR1), A46390 (DdcAR2), A46391 (DdcAR3), A54813 (DdcAR4), and AB045712 (TasA). (B) Phylogenetic analysis of cAR-like sequences. The tree shown was derived by maximum likelihood analysis and Bayesian inference and is drawn to scale, as indicated by the scale bar (0.1 substitutions per site). Thick lines indicate nodes with 1.00 Bayesian inference posterior probabilities and 100% mIBP support. An alternative branching pattern among the two deepest cAR nodes favored by mIBP is indicated by a double-headed arrow. Four putative G protein-coupled receptor sequences were used to root the tree. *N. crassa*. *Neurospora crassa*. GenBank accession nos.: AAM20722 (AtGPCR), AAO62367 (DdcR1A), EAA35706 (NcGPCR α), and EAA28751 (NcGPCR β). (C) Molecular phylogeny of Dictyostelids based on small subunit rRNA sequences. The tree shown was derived by using Bayesian inference and maximum likelihood analysis on 1,556 unambiguously aligned nucleotide positions. Sequences from solitary amoebae were used to root the tree.

DrcARII probe, which indicates that this gene is expressed only at very low levels, if at all.

To conclude, it appears that in the course of Dictyostelid evolution, the expression of a single *cARI*-type mRNA during culmination became supplemented with expression of a second mRNA from the same gene during preaggregative development.

Functional Analysis of the *D. minutum* cAR. The expression of *cARI* during *D. discoideum* and *D. rosarium* aggregation is fully

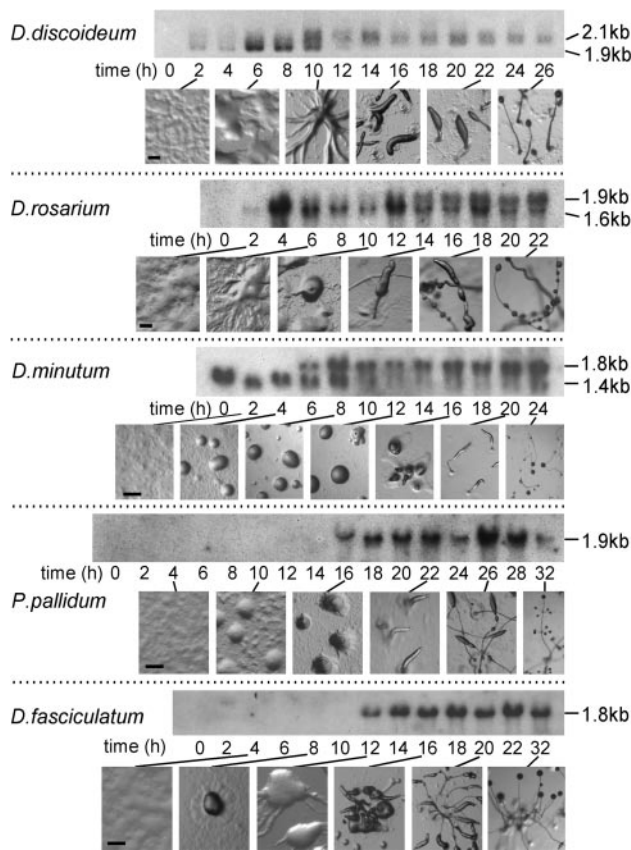


Fig. 2. Developmental regulation of cAR gene expression. Cells of the indicated five species were incubated on nonnutrient agar until fruiting bodies had formed. Total RNA was extracted at 2-h intervals, and the progression of development was photographed. Northern blots were probed at 65°C with [³²P]dATP-labeled *DdcAR1* cDNA or with the [³²P]dATP-labeled *DrcARI*, *DmcAR*, *PpcAR*, and *DfcAR* PCR products, respectively, and washed at high stringency. (Bar, 200 μ m.)

concordant with the fact that these species use cAMP to aggregate. However, the expression of a *cARI*-like gene during *D. minutum* aggregation is enigmatic in view of the fact that *D. minutum* cells use folate and not cAMP for aggregation (11). It is therefore particularly important to establish for this species that its cAR-like gene encodes a functional cAR. To do so, we cloned the full-length *DmcAR* gene from a *D. minutum* genomic DNA library and expressed it in the *D. discoideum* *carIcar3* mutant (18) for assay of cAMP-binding activity and functional complementation.

The library screen yielded three overlapping clones, which could be assembled into a 4,873-bp contig (Fig. 3A). In addition to the complete 1.16-kb *DmcAR* coding sequence, this contig also contained a complete second gene, which was named *DmDtmA*, and a gene fragment, which was named *DmSpkA*. BLAST searches of the entire GenBank protein database with these sequences identified the *D. discoideum* genes *DdSpkA* and *DDB02170155* as their most related orthologues. The *D. discoideum* genes occupy the same position relative to *DdcAR1* as their *D. minutum* orthologues to *DmcAR*. The flanking genes of *DdcAR2*, *DdcAR3*, and *DdcAR4* bear no similarity to the *DmcAR* flanking genes. This indicates that *DmcAR* is a true orthologue of *DdcAR1*, and that there is at least partial synteny between the *D. discoideum* and *D. minutum* genomes.

For heterologous expression of the *D. minutum* cAR in *D. discoideum*, we fused the *DmcAR* coding sequence to the constitutive *D. discoideum* A15 promoter in the extrachromosomal

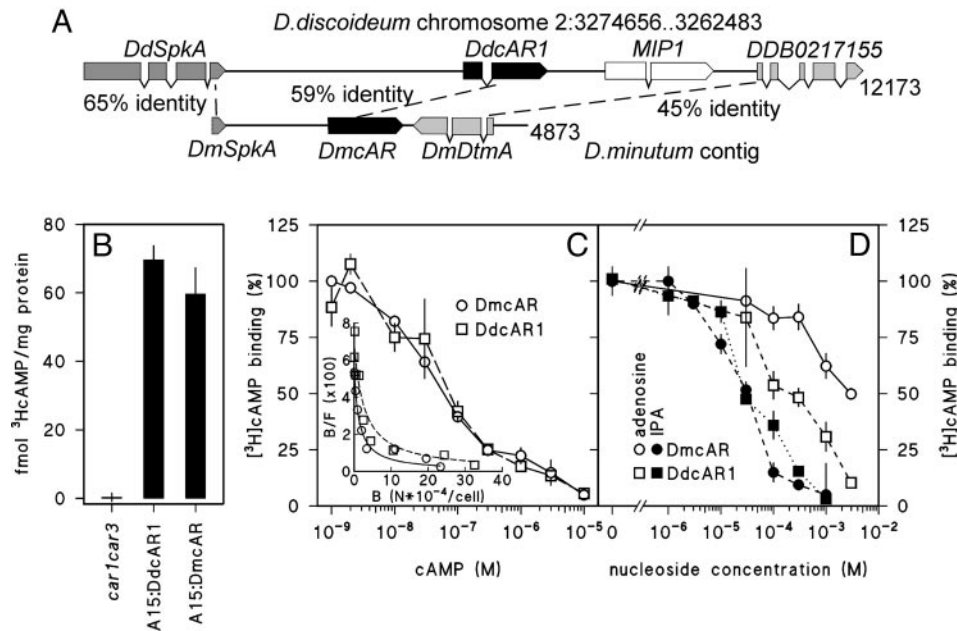


Fig. 3. Cloning and cAMP-binding properties of DmcAR. (A) Cloning of DmcAR. Screening of a *D. minutum* genomic DNA library with the *DmcAR* PCR product yielded a 4.87-kb contig of three clones. This contig contains *DmcAR* and two flanking genes, which we denote *DmSpkA* and *DmDtmA*. These genes are most similar to the *D. discoideum* genes *SpkA* and *DDB0217155*, respectively, which occupy the same positions relative to *DdcAR1* on chromosome 2 (36). The percentages of amino acid identity between the orthologous genes are indicated. (B) cAMP binding. *car1car3* cells, transformed with either *A15:DmcAR*, *A15:DdcAR1*, or no construct, were incubated with 10 nM [³H]cAMP and assayed for cell-surface-associated [³H]cAMP-binding activity. (C) Competition curve for cAMP. *A15:DmcAR*- or *A15:DdcAR1*-transformed *car1car3* cells were incubated with 1 nM [³H]cAMP and the indicated concentrations of cAMP and assayed for [³H]cAMP binding to the cell surface. The data are presented as percentage of [³H]cAMP binding in the absence of cAMP and as a Scatchard plot (37) (*inset*). B, bound; F, free cAMP; N, number of molecules. (D) Inhibition of [³H]cAMP binding by adenosine and 2′3′isopropylidene adenosine (IPA). The transformed cell lines were incubated with 10 nM [³H]cAMP and the indicated concentrations of adenosine and IPA and assayed for [³H]cAMP binding to the cell surface. The data are presented as percentage of [³H]cAMP binding in the absence of nucleosides. All data represent the means and SEM of two experiments performed in triplicate.

expression vector PJK1. The *A15:DmcAR* gene fusion was subsequently introduced into the *D. discoideum car1car3* mutant. This mutant lacks high-affinity receptors due to lesions in both its *cAR1* and *cAR3* genes and can consequently neither aggregate nor form fruiting bodies (18).

We first measured whether *A15:DmcAR* restored cell surface cAMP-binding activity in the *car1car3* mutant, using *car1car3* transformed with *A15:DdcAR1* as a control. Fig. 3B shows that cells transformed with *A15:DmcAR* or *A15:DdcAR1* bound significant amounts of [³H]cAMP, whereas the host *car1car3* strain bound none at all. Competition curves and Scatchard plots of [³H]cAMP binding (Fig. 3C) show that *DdcAR1* and *DmcAR* give rise to both high ($K_d \sim 30$ nM) and low ($K_d \sim 1$ μM) affinity-binding sites as reported for cAR1 in wild-type *D. discoideum* cells (28). The binding of cAMP to *DdcAR1*, but not to any of the other *D. discoideum* cARs, is inhibited by adenosine and more potently by the adenosine analog 2′3′isopropylidene adenosine (IPA) (19, 29). We investigated whether this was also the case for the *DmcAR*. Fig. 3D shows that both adenosine and IPA inhibit [³H]cAMP binding to *DmcAR*, although inhibition by adenosine occurs less effectively for *DmcAR* than for *DdcAR1*. In conclusion, these data show that the cAMP-binding properties of *DmcAR* are much more similar to those of *DdcAR1* than to any of the other *D. discoideum* cARs. This confirms the genetic evidence that *DmcAR* is a *DdcAR1* orthologue.

In addition to cAMP binding, a functional cAR should be able to interact with the downstream components of all cAMP-activated signal transduction pathways. We therefore examined whether *A15:DmcAR* can rescue the developmental defects of the *car1car3* mutant. Fig. 4A shows that transformation with *A15:DmcAR* restored aggregation and fruiting body formation

in *car1car3*, although there was a delay in aggregation of a few hours compared with the parent strain DH1 of the *car1car3* mutant.

During aggregation of *D. discoideum* cells, cAMP pulses are propagated in complex spiral wave patterns (30, 31). To investigate whether *DmcAR* can mediate similar complex behavior, we tracked the optical density waves that are diagnostic for pulsatile cAMP signaling during aggregation of *car1car3/A15:DmcAR* cells. The time-lapse movie represented in Fig. 4B shows spiral waves propagating from an aggregation center into a field of cells, which causes the cells to move toward the center. This indicates that *DmcAR* fully supports pulsatile cAMP signaling in *D. discoideum* and thus couples to the downstream components of the cAMP signaling machinery. Together with the biochemical data presented above, we therefore conclude that *DmcAR* is a functional high-affinity cAR.

The Role of cARs in Basal Dictyostelid Species. Similar to all investigated species in the most derived taxon group 4, *D. rosarium* uses cAMP as chemoattractant, but this is not the case for *D. fasciculatum*, *P. pallidum*, and *D. minutum*. What then is the function of cARs in these species? cAR1-mediated signaling adapts to sustained stimulation with cAMP or its nondegradable analog SpcAMPS; this feature enables cAR1 function to be pharmacologically abrogated by exposure to excess ligand (32, 33). Consistent with the known role of cAMP during *D. discoideum* aggregation, development on agar containing SpcAMPS inhibits aggregation of *D. discoideum* cells, thus mimicking the phenotype of *car1car3* cells. SpcAMPS can therefore be used to specifically determine which aspects of development, aggregation, fruiting body formation, or both, are regulated by cAMP signaling.

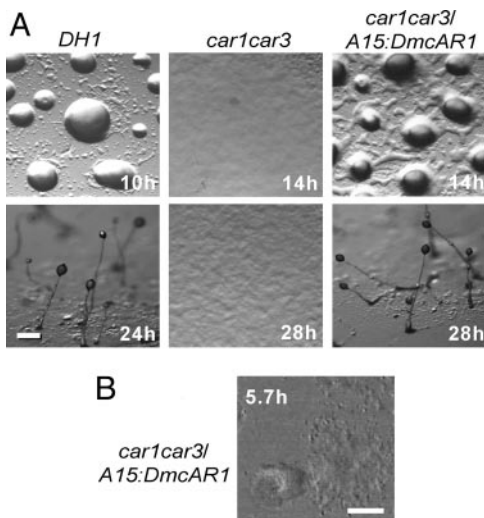


Fig. 4. Complementation of *Ddcar1car3* by *DmcAR*. (A) Restoration of development. The *D. discoideum car1car3* mutant, its parent DH1, and *car1car3* transformed with *A15:DmcAR* were incubated on nonnutrient agar at 22°C and photographed at 2-h intervals. (Bar, 100 μ m.) (B) Oscillatory signaling. *car1car3/A15:DmcAR* cells were incubated for 5 h at 4×10^5 cells per cm^2 on agar and subsequently tracked during 50 min at 10-s intervals by time-lapse videomicroscopy under phase-contrast illumination. Optical density waves were enhanced by image subtraction (30). The 256th video frame is shown. (Bar, 100 μ m.) See Movie 1, which is published as supporting information on the PNAS web site.

Fig. 5 shows that the development of all species was curtailed by SpcAMPS, although the manner in which this occurred differed among species. The most basal species, *D. fasciculatum*, aggregated normally with inflowing streams of cells when developing on SpcAMPS agar. However, although control aggregates rapidly developed into several robust upright culminants, the aggregates on SpcAMPS agar remained spread out and formed only small aberrant structures. Similarly, in neither *P. pallidum* nor *D. minutum* was the aggregation process itself affected by SpcAMPS. In *D. minutum*, the completed aggregates failed to form tips and thereafter dispersed. In *P. pallidum*, fruiting bodies were formed, but the majority of those were much reduced in size, and all fruiting bodies had lost the whorls of side branches that characterize this species. This phenotype was also reported for the *PpcAR* (*TasA*) null mutant (25), which shows that the SpcAMPS treatment mimics *cAR* gene disruption. In both *D. discoideum* and *D. rosarium*, SpcAMPS blocked the aggregation process, consistent with the fact that both species use cAMP to aggregate. These experiments show that the basal species *D. fasciculatum*, *P. pallidum*, and *D. minutum* use dynamic cAMP signaling only during fruiting body formation. This is in contrast to the more derived species *D. discoideum* and *D. rosarium*, which additionally use cAMP signaling for the aggregation process.

Discussion

We identified orthologues of the *D. discoideum* chemotactic *cAR1* in four species, *D. fasciculatum*, *P. pallidum*, *D. minutum*, and *D. rosarium*. With the exception of *D. rosarium*, none of these species uses cAMP as chemoattractant for aggregation. The *D. minutum cAR* can nevertheless fully rescue chemotactic cAMP signaling and aggregation when expressed in a *D. discoideum* mutant that lacks high-affinity *cARs*.

D. minutum, *P. pallidum*, and *D. fasciculatum* each represent earlier branches off the main line of descent leading to the taxon group that includes *D. discoideum* and *D. rosarium* (Fig. 1C) (P.S. and S.L.B., unpublished work). In contrast to *D. discoideum* and

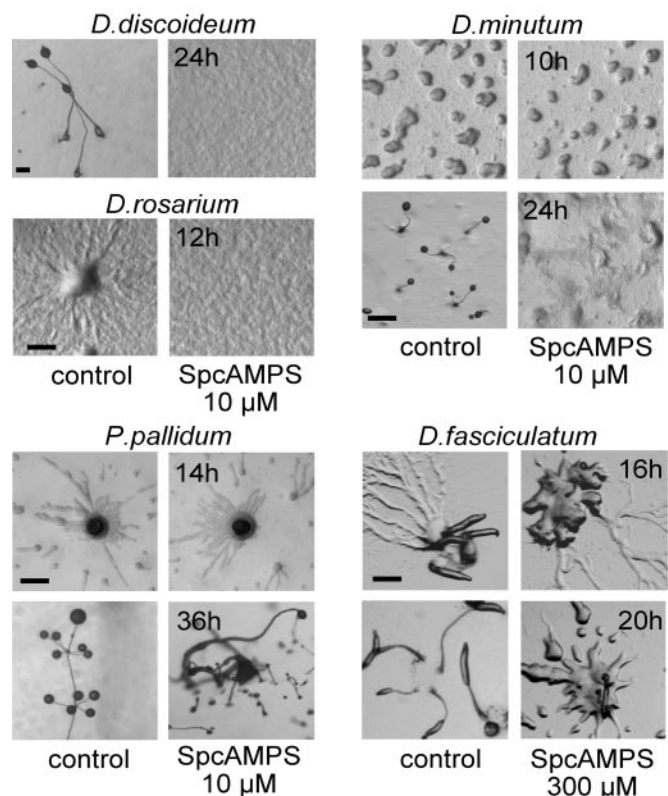


Fig. 5. Effects of SpcAMPS on *Dictyostelid* development. Cells from the indicated species were distributed at 2×10^5 cells per cm^2 on nonnutrient agar (control) or agar with 10 or 300 μ M SpcAMPS and incubated at 22°C. The progression of development was photographed at 2-h intervals. (Bar, 200 μ M.)

D. rosarium, two of these species express *cAR1* only during fruiting body formation (Fig. 2). In all three species, only fruiting body formation, and not aggregation, is disrupted when *cAR* function is blocked (25) (Fig. 5). This strongly suggests that coordination of fruiting body morphogenesis is the ancestral function of extracellular cAMP signaling, and that its more commonly known role in *D. discoideum* and *D. rosarium* aggregation is evolutionarily derived. In *D. discoideum*, cAMP also triggers postaggregative gene expression (10). Once suitable marker genes are identified for the basal species, it will be of great interest to establish whether this aspect of extracellular cAMP signaling also has ancient roots.

The spiral waves of cell movement that are triggered by cAMP oscillations in a field of starving *D. discoideum* cells are one of the most striking examples of self organization in biology. We now show that they also represent a stunning example of a derived evolutionary novelty. How might this novel feature have come about? The promoter structure of cAMP signaling genes in *D. discoideum* suggests a mechanistic explanation for this alteration. The gene encoding the extracellular cAMP phosphodiesterase, *PdsA*, has three separate promoters for expression during growth, aggregation, and fruiting body (late) morphogenesis, respectively. The late promoter is proximal to the coding sequence, followed by the growth-specific promoter and finally the aggregation promoter (34). The *DdcAR1* gene has two separate promoters: the late promoter, proximal to the coding sequence, is for expression during fruiting body formation, whereas the aggregation promoter is distal to the late promoter (26). We hypothesize that the proximal promoters direct the ancestral function of the cAMP signaling genes in fruiting body

morphogenesis, whereas the distal promoters were acquired later to accommodate the derived roles of cAMP in early development.

Pathway cooption through the acquisition of novel promoter elements is not the entire story, as evidenced by the intermediate species *D. minutum*, which shows altered *cAR* gene expression but lacks aggregation to cAMP. The *D. minutum cAR* encodes a fully functional cAR, which suggests that aggregation to cAMP has not been lost in *D. minutum*. Rather, we propose that aggregation to cAMP has not yet been fully gained. This could have several causes: (i) the recruited pathway might not be completely coupled to the downstream effectors and (ii) other components required for chemotactic signaling, such as adenylyl cyclase A and PdsA, may not yet be expressed during aggregation. In fact, the high expression of the *D. minutum cAR* during growth suggests that it may serve a function in food seeking, because the bacterial food source is known to secrete cAMP (35). As a transitory phase in the sequence of events that lead to cooption of cAMP signaling for aggregation, food seeking has the advantage of requiring only cAMP detection and not oscillatory cAMP production.

The cAMP signaling system in the Dictyostelids is composed of at least three major parts: cAMP production by adenylyl cyclases, detection by cARs, and degradation by specific phosphodiesterases. Here, just one part of this apparatus is considered, but future work will seek to elucidate the route taken toward the use cAMP in aggregation by considering each component independently and then all together. Through this approach, we hope to begin to understand the molecular origins of new traits via gene recruitment.

We thank Jim C. Cavender (Ohio University, Athens), Guenther Gerisch (Max Planck Institute, Martinsried, Germany), and Hiromitsu Hagiwara (National Science Museum, Tokyo) for their kind gifts of *D. fasciculatum* SH3, *D. minutum* 71-2, *P. pallidum* TNS-C-98, and *D. rosarium* M45, respectively. We thank Peter Devreotes (Johns Hopkins University Medical School, Baltimore) for the gifts of the PJK1 and A15:DdcAR1 vectors and Robert Insall (University of Birmingham, Birmingham, U.K.) for the *car1car3* cell line. We are grateful to Dirk Dormann (University of Dundee, Dundee, U.K.) for advice on time-lapse video-microscopy. This research was supported by Biotechnology and Biological Sciences Research Council Grants 94/COD16760 and 94/COD16761, Wellcome Trust Grant 057137, and a National Sciences Foundation postdoctoral fellowship (to D.E.R.).

- Long, M., Betran, E., Thornton, K. & Wang, W. (2003) *Nat. Rev. Genet.* **4**, 865–875.
- True, J. R. & Carroll, S. B. (2002) *Annu. Rev. Cell Dev. Biol.* **18**, 53–80.
- Lee, P. N., Callaerts, P., de Couet, H. G. & Martindale, M. Q. (2003) *Nature* **424**, 1061–1065.
- Irish, V. F. (2003) *BioEssays* **25**, 637–646.
- Raper, K. B. (1984) *The Dictyostelids* (Princeton Univ. Press, Princeton).
- Konijn, T. M., Van De Meene, J. G., Bonner, J. T. & Barkley, D. S. (1967) *Proc. Natl. Acad. Sci. USA* **58**, 1152–1154.
- Siegert, F. & Weijer, C. J. (1992) *Proc. Natl. Acad. Sci. USA* **89**, 6433–6437.
- Pitt, G. S., Milona, N., Borleis, J., Lin, K. C., Reed, R. R. & Devreotes, P. N. (1992) *Cell* **69**, 305–315.
- Lacombe, M.-L., Podgorski, G. J., Franke, J. & Kessin, R. H. (1986) *J. Biol. Chem.* **261**, 16811–16817.
- Devreotes, P. N. (1994) *Neuron* **12**, 235–241.
- De Wit, R. J. W. & Konijn, T. M. (1983) *Cell Differ.* **12**, 205–210.
- Shimomura, O., Suthers, H. L. B. & Bonner, J. T. (1982) *Proc. Natl. Acad. Sci. USA* **79**, 7376–7379.
- Cocucci, S. & Sussman, M. (1970) *J. Cell Biol.* **45**, 399–407.
- Don, R. H., Cox, P. T., Wainwright, B. J., Baker, K. & Mattick, J. S. (1991) *Nucleic Acids Res.* **19**, 4008–4008.
- Sun, B., Ma, H. & Firtel, R. A. (2003) *Mol. Biol. Cell* **14**, 4526–4540.
- Nellen, W., Datta, S., Reymond, C., Sivertsen, A., Mann, S., Crowley, T. & Firtel, R. A. (1987) in *Methods in Cell Biology*, ed. Spudich, J. A. (Academic, Orlando, FL), Vol. 28, pp. 67–100.
- Sambrook, J. & Russell, D. (2001) *Molecular Cloning: A Laboratory Manual* (Cold Spring Harbor Lab. Press, Plainview, NY).
- Insall, R. H., Soede, R. D. M., Schaap, P. & Devreotes, P. N. (1994) *Mol. Biol. Cell* **5**, 703–711.
- Verkerke-VanWijk, I., Kim, J. Y., Brandt, R., Devreotes, P. N. & Schaap, P. (1998) *Mol. Cell Biol.* **18**, 5744–5749.
- Thompson, J. D., Gibson, T. J., Plewniak, F., Jeanmougin, F. & Higgins, D. G. (1997) *Nucleic Acids Res.* **25**, 4876–4882.
- Ronquist, F. & Huelsenbeck, J. P. (2003) *Bioinformatics* **19**, 1572–1574.
- Felsenstein, J. (2004) PHYLIP Phylogeny Interference Package (Univ. of Washington, Seattle), Version 3.6b.
- Jones, D. T., Taylor, W. R. & Thornton, J. M. (1992) *Comput. Appl. Biosci.* **8**, 275–282.
- Strimmer, K. & Von Haeseler, A. (1996) *Mol. Biol. Evol.* **13**, 964–969.
- Kawabe, Y., Kuwayama, H., Morio, T., Urushihara, H. & Tanaka, Y. (2002) *Gene* **285**, 291–299.
- Louis, J. M., Saxe, C. L., III, & Kimmel, A. R. (1993) *Proc. Natl. Acad. Sci. USA* **90**, 5969–5973.
- Saxe, C. L., III, Johnson, R. L., Devreotes, P. N. & Kimmel, A. R. (1991) *Genes Dev.* **5**, 1–8.
- Henderson, E. J. (1975) *J. Biol. Chem.* **250**, 4730–4736.
- Van Lookeren Campagne, M. M., Schaap, P. & Van Haastert, P. J. M. (1986) *Dev. Biol.* **117**, 245–251.
- Tomchik, K. J. & Devreotes, P. N. (1981) *Science* **212**, 443–446.
- Siegert, F. & Weijer, C. J. (1995) *Curr. Biol.* **5**, 937–943.
- Rossier, C., Gerisch, G., Malchow, D. & Eckstein, F. (1978) *J. Cell Sci.* **35**, 321–338.
- Van Haastert, P. J. M. & Van der Heijden, P. R. (1983) *J. Cell Biol.* **96**, 347–353.
- Faure, M., Franke, J., Hall, A. L., Podgorski, G. J. & Kessin, R. H. (1990) *Mol. Cell Biol.* **10**, 1921–1930.
- Konijn, T. M., van de Meene, J. G. C., Chang, Y. Y., Barkley, D. S. & Bonner, J. T. (1969) *J. Bacteriol.* **99**, 510–512.
- Klein, P. S., Sun, T. J., Saxe, C. L., III, Kimmel, A. R., Johnson, R. L. & Devreotes, P. N. (1988) *Science* **241**, 1467–1472.
- Glockner, G., Eichinger, L., Szafranski, K., Pachebat, J. A., Bankier, A. T., Dear, P. H., Lehmann, R., Baumgart, C., Parra, G., Abril, J. F., et al. (2002) *Nature* **418**, 79–85.
- Scatchard, G. (1949) *Ann. N.Y. Acad. Sci.* **51**, 660–672.